BIAS-FIELD/FREQUENCY DESIGN CHARTS FOR COMPOSITE GYROTROPIC RESONATORS

Sheikh S.I., Gibson A.A.P. and Dillon B.M.

University of Manchester Institute of Science and Technology
P.O. Box 88, Manchester M60 1QD, United Kingdom

ABSTRACT

The permeability and permittivity tensors of magnetised ferrite and semiconductor materials have different dependencies on bias field, signal frequency and material properties. Mode charts are presented for composite planar ring resonator junctions: the semiconductor case has an additional resonance region and exhibits more symmetrical split frequencies than the ferrite.

INTRODUCTION

Gyrotropic behaviour in magnetically biased, microwave ferrites is governed by the Polder permeability tensor[1]. The analytic procedure of substituting this tensor into Maxwell's equation is well understood and design techniques for phase shift and control components have been widely disseminated[2]. Commercially available ferrites can be used to produce useful non-reciprocal effects up to around 40 GHz. Above this frequency range the gyrotropic properties of semiconductor materials are being investigated for use in non-reciprocal devices such as planar circulators[4]. The analysis is based on the Drude model of electromagnetic propagation through a magnetically biased plasma. Before a semiconductor circulator can be designed with confidence the splitting characteristics of the resonator junction should be compared with the predicted mode charts. The split frequency solutions shown in the mode charts also underpins the bandwidth and loss performance of the device.

A comparative study of the theoretical mode charts is presented for the dielectric-ferrite (DF) and dielectric-semiconductor (DS) ring resonators. Compared to homogeneous structures this geometry provides additional variables, flexibility and opportunities for novel multiport components[5]. The study is undertaken in the frequency/bias-field plane as this provides a clear illustration of the lossy resonance regions and the normal mode splitting in terms of experimental parameters. Solutions in this plane do not reflect the dualities of the original semiconductor and ferrite tensors. For ferrites the most symmetrical wideband split is known to occur at frequencies below ferrimagnetic resonance. In semiconductors excellent symmetrical splitting is predicted in the bias region that falls between the two extraordinary-wave resonances.

METHOD OF ANALYSIS

Gyrotropic planar junctions are usually immersed in a static magnetic field perpendicular to the direction of signal propagation. For an axially directed ($\hat{z}$) field, ferrites yield a tensor permeability and semiconductors a tensor permittivity both of the form,

$$\begin{bmatrix} p & -jq & 0 \\ jq & p & 0 \\ 0 & 0 & r \end{bmatrix} \quad (1)$$

TH 3F

0-7803-3246-6/96/$5.00 © IEEE

For ferrites, p, q and r are nonlinear functions of signal frequency (f), applied field (H_o), material magnetization (M), axial demagnetizing factor (N_z) and the gyromagnetic ratio (γ) of the material. The continuous value of M and N_z for both saturated and partially magnetised ferrites are calculated using a magnetization model enunciated elsewhere[6,7]. In the case of magnetized semiconductors[3,4] p, q and r are nonlinear functions of the relative dielectric constant (ϵ_r), the number of electrons per unit volume (N), the charge of an electron (e) and the constant effective mass (m^*) of the material.

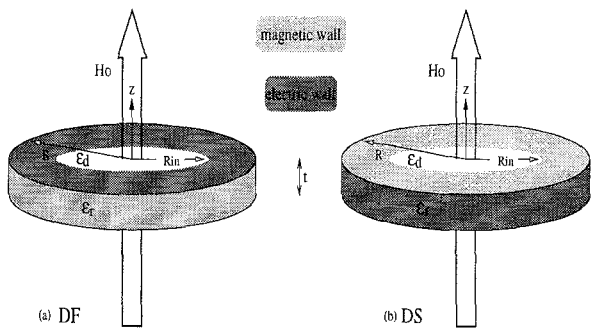

Figure 1: Schematic diagram of planar axisymmetric inhomogeneous dielectric-ferrite and dielectric-semiconductor resonators.

The composite structures schematically illustrated in figure 1 are the planar DF resonator and its dual DS configuration associated with circulation action. Assuming no field variation in the axial direction ($\frac{\partial}{\partial z} = 0$), the modes can be classified as either TE or TM. The material tensors can be substituted into Maxwell's equations and solved using the boundary conditions of figure 1 to produce dual characteristic equations (CE) for each geometry. For ferrites the CE is expressed in terms of an effective permeability (μ_{eff}) given by,

$$\mu_{eff} = \frac{p^2 - q^2}{p} \qquad (2)$$

$$= \frac{\gamma^2(H_o - M\ N_z)^2 - f^2 + 2\ \gamma^2(H_o - M\ N_z)M + (\gamma\ M)^2}{\gamma^2(H_o - M\ N_z)^2 - f^2 + \gamma^2(H_o - M\ N_z)M}$$

and the ratio of the off diagonal to main diagonal tensor permeability entries,

$$\frac{q}{p} = \frac{\gamma\ M\ f}{\gamma^2(H_o - MN_z)^2 - f^2 + \gamma^2(H_o - MN_z)M} \qquad (3)$$

The dual CE for semiconductors is also written as a function effective permittivity (ϵ_{eff}) and the ratio of tensor permittivity components defined as,

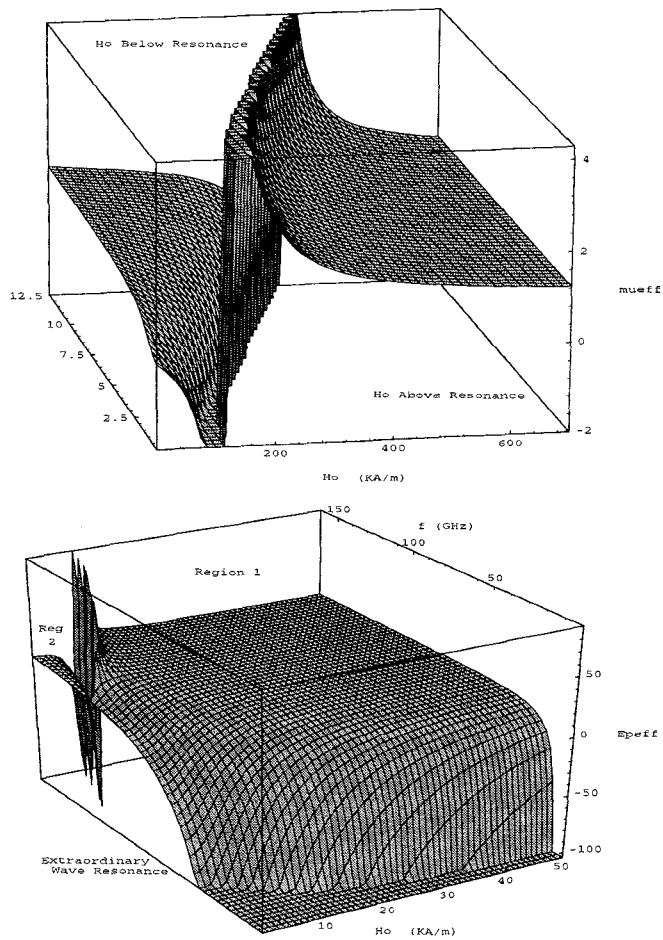

Figure 2: (a) Effective permeability of ferrites and (b) effective permittivity of semiconductors as a function of bias field and signal frequency.

$$\epsilon_{eff} = \frac{p^2 - q^2}{p} \qquad (4)$$

$$= \frac{\epsilon\ f^2\left\{\epsilon\left((f\ m^*)^2 - (e\ \mu_o\ H_o)^2\right) - 2\ N\ e^2\ m^*\right\} + \{N\ e^2\}^2}{\epsilon_o\ f^2\left\{\epsilon\left((f\ m^*)^2 - (e\ \mu_o\ H_o)^2\right) - N\ e^2\ m^*\right\}}$$

$$\frac{q}{p} = \frac{N\ |e^3|\ \mu_o\ H_o}{f\left\{\epsilon\left((fm^*)^2 - (e\ \mu_o\ H_o)^2\right) - N\ e^2\ m^*\right\}} \quad (5)$$

where $\epsilon = \epsilon_o\ \epsilon_r$. It is clear from equations (2) and (3) against (4) and (5) that the frequency/bias-field solutions do not reflect the original duality suggested by figure 1 and the characteristic equations expressed in terms of the tensor entries of equation 1.

DISCUSSIONS AND RESULTS

Figure 2 illustrates the effective permeability (2) of ferrites and effective permittivity (4)

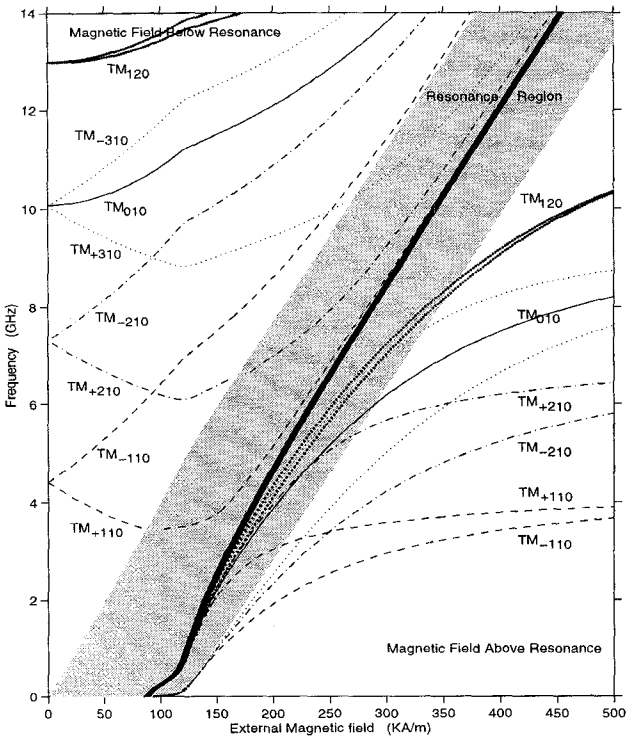

Figure 3: Applied field/frequency solution of a composite DF (YIG G113) resonator over the three regions of magnetization.(M_s=140 $\frac{KA}{m}$, ϵ_r=15.9, ϵ_d=1, R_{out}=5 mm, R_{in}=1 mm, t=1 mm)

of semiconductors as a function of the experimental variables: bias field and signal frequency. Microwave ferrite devices can be biased to operate either above or below the single ferrimagnetic resonance. In semiconductors there are two resonance regions predicted

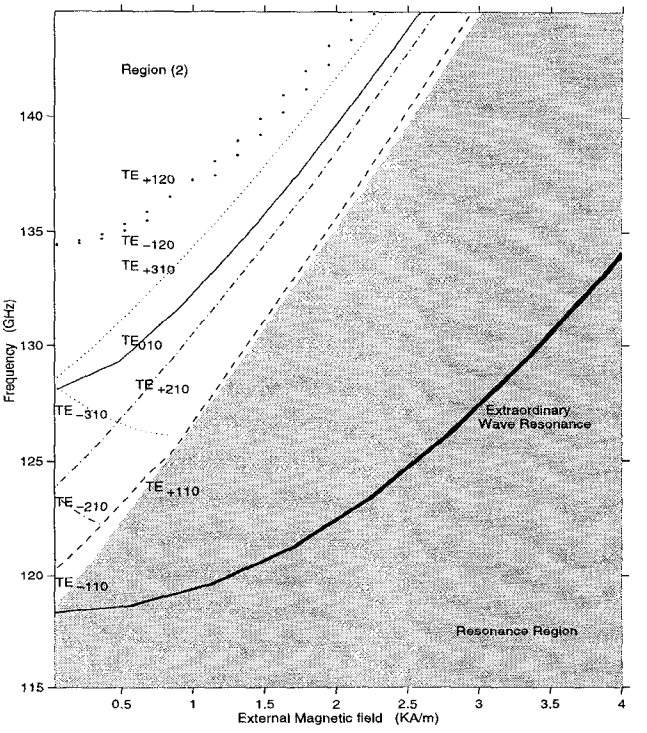

Figure 4: Mode charts for a DS (InSb) planar resonator, biased between the two extraordinary-wave resonances.(N=10^{18} $\frac{1}{m^3}$, $\frac{m^*}{m_e}$=0.014, ϵ_r=16, $Temp$ = $77K$, R_{out}=1mm, R_{in}=0.2mm, t=0.1mm)

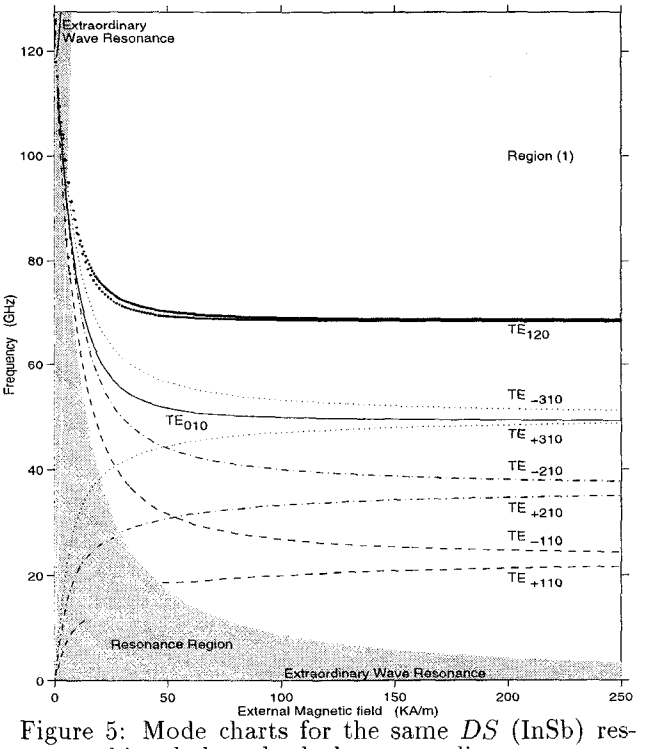

Figure 5: Mode charts for the same DS (InSb) resonator, biased above both the extraordinary-wave resonances.

by the Drude model. These regions are associated with coupling to the so called extraordinary waves and the main bias region falls between these two resonances. For both materials, damping losses occur in all the resonance regions.

The resonant frequencies of the geometries in figure 1 can be presented as a continuous function of applied field. Figure 3 displays the mode chart of a planar DF (YIG $G113$) composite resonator, with the shaded area representing the lossy ferrimagnetic resonance region. It is evident from this figure that operation below resonance exhibits more symmetrical wideband characteristics than the corresponding above resonance region. The applied-field/frequency response of a DS ($InSb$) structure is illustrated in figures 4 and 5. The normal modes depicted in region 1 of figure 4 predicts excellent symmetrical splitting characteristics suitable for planar circulator and tunable filter operation. Figure 5 displays a subsidiary operating region ($Reg.2$) at frequencies above both the extraordinary-wave resonances.

Table 1: Effect on the modal behavior with changing dimensions and material properties.

Increasing value of	Frequency Splitting		Onset Frequency	
YIG G113-Air Composite Resonator				
	Above Resonance	*Below Res.*	$TM_{\pm nm0}$ *modes* *Above Res*	*Below Res*
R_{out}	reduces		reduces	
R_{in}	reduces		reduces	
ϵ_r	reduces		reduces	
M	increases		reduces	no change
ϵ_d	increases		reduces	
InSb-Air Composite Resonator				
	Region 1 (fig 4)	*Region 2* (fig 5)	$TE_{\pm nm0}$ *modes* *Reg 1*	*Reg 2*
R_{out}	increases	reduces	reduces	
R_{in}	reduces		reduces	
ϵ_r	reduces		reduces	
N	increases		reduces	increases
m^*	reduces		reduces	
ϵ_d	increases		reduces	increases

CONCLUSIONS

Figures 3, 4 and 5 provide illustrative examples of normal mode splitting in composite ferrite and semiconductor axisymmetric planar resonators. Table 1 summarises the effect on these modal behavior of changing geometrical and material parameters of the device.

References

[1] Polder, D., "On the Theory of Ferromagnetic Resonance", Phil. Mag., Vol.40, pp 95-115, 1949.

[2] Baden Fuller A.J., "Ferrites ar Microwave Frequencies", Perer Peregrinus Ltd., Chapter 7-10, 1987.

[3] Davis L.E. and Sloan R., "Predicted Performance of Semiconductor Circulator with Losses", IEEE Trans on Microwave Theory and Techs., Vol.41, No.12, Dec. 1993.

[4] Special Issue on Gyroelectric Materials, IEE Proc,Pt.H, Vol.140,No.3, June 1993

[5] Dmitryev V.A. and Davis L.E., "Nonreciprocal Devices using Ring Resonators", IEE Proc., Pt.H, Vol.139, pp 257-263, June 1992.

[6] Hansson B. and Fillipsson G., "Microwave Circulators in Stripline and Microstrip Techniques", Chalmers University of Technology, Sweden, 1976.

[7] Green J.J. and Sandy F., "Microwave Characterization of Partially Magnetised Ferrite", IEEE Trans on Microwave Theory and Techs., Vol.22, pp 641, 1974.

[8] Gibson A.A.P., Dillon B.M. and Sheikh S.I., "Applied Field/Frequency Response of Planar Gyromagnetic Disks", Int. J. Electronics, Vol.76, No., pp 1073, 1994.